



RESEARCH

# Forecasting carbon dioxide emissions in Chongming: a novel hybrid forecasting model coupling gray correlation analysis and deep learning method

Yaqi Wang · Xiaomeng Zhao · Wenbo Zhu ·  
Yumiao Yin · Jiawei Bi · Renzhou Gui

Received: 27 April 2024 / Accepted: 6 September 2024 / Published online: 17 September 2024  
© The Author(s), under exclusive licence to Springer Nature Switzerland AG 2024

**Abstract** Predicting regional carbon dioxide (CO<sub>2</sub>) emissions is essential for advancing toward global carbon neutrality. This study introduces a novel CO<sub>2</sub> emissions prediction model tailored to the unique environmental, economic, and energy consumption of Shanghai Chongming. Utilizing an innovative hybrid approach, the study first applies grey relational analysis to evaluate the influence of economic activity, natural conditions, and energy consumption on CO<sub>2</sub> emissions. This is followed by the implementation of a dual-channel pooled convolutional neural network (DCNN) that captures both local and global features of the data, enhanced through feature stacking. Gated recurrent unit (GRU) network then assesses the temporal aspects of these features, culminating in precise

CO<sub>2</sub> emission predictions for the region. The results indicate: (1) The proposed hybrid model achieves accurate predictions based on accounting data, with high precision, low error, and good stability. (2) The study found an overall increase in Chongming's carbon emissions from 2000 to 2022, with the prediction results being generally consistent with existing research findings. (3) The proposed method, based on Chongming's CO<sub>2</sub> emission predictions, addresses issues such as the scarcity of effective accounting data and inaccuracies in traditional calculation methods. The results can provide effective technical support for local government policies on carbon reduction and promote sustainable development.

Y. Wang · X. Zhao · W. Zhu · Y. Yin · J. Bi · R. Gui  
College of Electronic and Information Engineering, Tongji University, Shanghai 201804, China  
e-mail: wangyaqi@tongji.edu.com

X. Zhao  
e-mail: 2011234@tongji.edu.cn

W. Zhu  
e-mail: wzbzu@tongji.edu.cn

Y. Yin  
e-mail: 2232927@tongji.edu.cn

J. Bi  
e-mail: jiaweibi@tongji.edu.cn

R. Gui (✉)  
Institute of Carbon Neutrality, Tongji University, Shanghai 200092, China  
e-mail: rzgui\_eie@163.com

**Keywords** Carbon neutrality · Carbon dioxide emission forecasting · Grey correlation analysis · Dual-channel convolutional neural network · Gated recurrent unit

## Introduction

Since the Industrial Revolution, human activities have led to a sharp increase in CO<sub>2</sub> emissions, which has triggered the greenhouse effect and resulted in global warming (Muruganandam et al., 2023). According to the Copenhagen Diagnosis, global temperatures are expected to rise by 7 °C by 2100, with sea levels rising over 1 m (Song et al., 2023). Severe climate change not only results in more frequent extreme weather events

such as heatwaves, cold spells, and hurricanes (Tong et al., 2022), but also severely damages ecosystems, leading to reduced crop yields, water scarcity, and ocean acidification, posing various severe threats to human life (Wang et al., 2023).

Controlling CO<sub>2</sub> emissions has become a global consensus. According to the goals of the Paris Agreement, nations have set specific emission reduction targets and implemented corresponding measures to mitigate the impacts of climate change on ecosystems and human socio-economic development (Xu et al., 2024). In 2022, China accounted for 32.9% of global carbon emissions (Wu et al., 2023), making it the largest emitter worldwide (Jiang et al., 2023). In response, China has implemented various measures and policies, such as effectively controlling greenhouse gas emissions in key industrial sectors, promoting green and low-carbon development in urban and rural construction, establishing a green and low-carbon transportation system, and continuously enhancing ecological carbon sequestration capabilities, significantly reducing its greenhouse gas emissions (Liao et al., 2021).

Predicting CO<sub>2</sub> emissions is crucial for controlling emissions. Understanding the dynamic trends of CO<sub>2</sub> emissions can provide a theoretical basis for formulating and implementing emission reduction policies. However, compared to global and national prediction, regional CO<sub>2</sub> emission prediction is more susceptible to factors such as geography, regional economy, industry, and population structure (Feng et al., 2012), leading to difficulties due to data insufficiency and low correlation of accounting indicators when using traditional methods for regional emission accounting, thus increasing the complexity of predictions. Consequently, there is an urgent need to develop a quantitative model that can accurately predict regional CO<sub>2</sub> emission trends to guide the decision-making for regional emission policies. This study uses Chongming, Shanghai as a case study.

## Literature review

CO<sub>2</sub> emission prediction models are designed to predict the volume of CO<sub>2</sub> emissions over a specific future period. Existing studies are categorized into three types: statistical and econometric models, grey models, and nonlinear artificial intelligence models.

In the realm of statistical and econometric models, researchers frequently employ statistical or econometric methods to quantitatively assess CO<sub>2</sub> emissions. For instance, Wen et al. (2022) analyzed scenarios for China to achieve carbon neutrality using the STIRPAT and system dynamics models, identifying eight pathways that align with China's current carbon neutrality goals. Liu et al. (2023a) quantified the spatio-temporal dynamics and drivers of county-level carbon emissions in China from 2000 to 2020, using exploratory spatio-temporal data analysis and spatial econometrics based on remote sensing imagery datasets. Zeng and Yi (2023) combined scenario analysis with the STIRPAT model to construct a logistic growth model, studying time-series data of CO<sub>2</sub> emissions in twenty-six urban areas to inform peak emission pathways for China. Raza (2022) employed the autoregressive distributed lag (ARDL) model to examine the relationship between CO<sub>2</sub> emissions and their determinants in Pakistan, analyzing both long-term and short-term effects and discovering a bidirectional causal relationship. However, the considerable reliance of statistical and econometric methods on sample data substantially constrains their application scope.

The grey model is an effective forecasting method for situations with small data sample sizes and incomplete data, categorized into univariate and multivariate grey forecasting models (Kang et al., 2022; Yu et al., 2021). In recent years, the use of grey models for forecasting and analyzing CO<sub>2</sub> emissions has become a focal point of research (Duan & Pang, 2021). For example, Wang and Zhang (2022) utilized carbon emission data from thirty provinces in China to establish a spatial grey model, SGM(1,1,m), forecasting CO<sub>2</sub> emissions from 2020 to 2025. The results demonstrated the efficacy of the SGM(1,1,m) model in capturing the spatial correlations of carbon emissions. Zhou et al. (2021) applied a mean attenuation buffering operator to handle historical data, implementing a grey rolling mechanism based on the principle of prioritizing new information, to forecast China's CO<sub>2</sub> emission trends. The proposed model demonstrated improved simulation and forecasting performance, with high stability. Wang et al. (2022) utilized an improved gray multivariate convolutional integral model (AGMC(1, N)) to predict carbon emissions in Shanxi Province, China, and achieved robust prediction outcomes. Ding et al. (2020) introduced a discrete grey power model combined with a leading rolling mechanism to forecast energy-related CO<sub>2</sub> emissions

in China from 2011 to 2015. This model significantly outperformed other baseline models across three performance metrics. However, in current CO<sub>2</sub> emission predictions, closely related data such as ecological environment, socioeconomic factors, and population continue to be updated and expanded. These datasets exhibit characteristics like nonlinear growth, high volatility, and rapid iterative updates, thereby posing limitations on the adaptability of grey models in dynamic environments (Ding & Li, 2021; Duan et al., 2024).

Nonlinear artificial intelligence models uncover the complex patterns and nonlinear trends between CO<sub>2</sub> emission factors and emission volumes. For instance, Faruque et al. (2022) utilized convolutional neural networks-long short-term memory (CNN-LSTM), CNN, LSTM, and dense neural networks (DNN) to explore the relationships among CO<sub>2</sub> emissions, GDP, and energy consumption in Bangladesh, finding that the DNN model performed the best. Ahmadi et al. (2023) employed artificial neural networks and the group method of data handling to identify the most significant carbon emissions among greenhouse gases, based on varied energy shares of the primary energy supply and GDP as an indicator of economic activity. Saleh et al. (2016) employed the support vector machine model to predict CO<sub>2</sub> emissions, tracking emissions based on the amount of electricity used in the production process and during coal combustion. Zhang et al. (2021) used a backpropagation-based neural network to estimate carbon emissions in urban blocks, demonstrating higher accuracy compared to other methods. Han et al. (2023) employed a hybrid model combining LSTM and CNN to precisely forecast carbon emissions across thirty provinces in China. The results indicated that this model outperformed other models in terms of predictive performance. The application of nonlinear artificial intelligence models is a current research hotspot.

In summary, grey models excel in scenarios involving small-sample data predictions, characterized by linear features, ease of modification, and strong predictive capabilities. Nonlinear artificial intelligence models, by integrating spatio-temporal data characteristics, provide optimal feature representations for carbon emission prediction models due to their robust nonlinear data-fitting capabilities. Building on the previously discussed models, this study proposes a hybrid model, GDCNN-GRU, which combines grey relational analysis and GRU networks within a parallel DCNN framework, to predict CO<sub>2</sub> emissions in Chongming.

## Contribution and organization

This paper seeks to develop the hybrid model for the quantitative forecasting of CO<sub>2</sub> emissions in Chongming. The contributions of this paper are summarized as follows.

- The grey relational model is utilized to examine the interconnections between socio-economic development, energy consumption, natural environment data, and CO<sub>2</sub> emissions. Through grey relational analysis, the experimental results reveal a significant nonlinear relationship between these factors and CO<sub>2</sub> emissions in Chongming.
- DCNN framework was constructed to explore the local and global characteristics of factors influencing CO<sub>2</sub> emissions in Chongming. Additionally, GRU was employed to investigate the temporal dependencies of these features, analyzing the complex spatio-temporal relationships between Chongming's influencing factors and CO<sub>2</sub> emissions.
- Integrating grey relational analysis, DCNN structure, and GRU, a new model named GDCNN-GRU, was developed for predicting CO<sub>2</sub> emissions in Chongming. The proposed model was compared in terms of performance with single models such as CNN, LSTM, MLP, and BiLSTM, their combinations, and hybrid models incorporating grey relational analysis. The results indicate that the proposed model has superior predictive performance. In the CO<sub>2</sub> emission predictions for 2015 to 2017, the proposed model exhibited prediction errors specifically of 1.096%, 0.931%, and 0.584%. In the baseline comparison experiments, the proposed model demonstrates superior stability and predictive accuracy compared to other models. Relative to existing research, it exhibits higher precision and better stability, with potential for future application in predicting CO<sub>2</sub> emissions across different regions.

The structure of this paper is organized as follows. The “[Introduction](#)” section is the introduction. The “[Materials and methods](#)” section describes the case study, data sources, and related methods, elaborating on the proposed model's structure and model evaluation metrics. The “[Experimental results and analysis](#)” section presents the experimental results and provides an analysis of these results. The “[Conclusion](#)” section summarizes the main findings of the study and potential future research directions.

## Materials and methods

### Case descriptions and data sources

This paper focuses on Chongming in Shanghai as the subject of study. Located at the confluence of the Yangtze River and the East China Sea, Chongming consists of Chongming Island, Changxing Island, and Hengsha Island, as illustrated in Fig. 1. As the world's largest alluvial island at a river estuary, Chongming Island covers an area of 1413 square kilometers (Wang et al., 2018). Since 2001, the Chongming government has aimed to improve the overall ecological environment of Shanghai, initiating the region's first carbon neutrality action plan to develop a globally influential carbon-neutral ecological island (Cai et al., 2020; Guo et al., 2023). However, Chongming's economic development started later, and reliable indicators for carbon emission forecasting are scarce, making predictions challenging. To this end, this study aims to predict regional CO<sub>2</sub> emissions in Chongming, addressing the issue of inaccurate predictions due to scarce data, furthering climate governance, establishing emission reduction measures, and aiding in the development of a world-class ecological island.

### Experimental datasets

This study collected data on the natural environment, socio-economic factors, and energy consumption in

Chongming, covering the period from 2002 to 2022 and including 26 specific indicators. The statistical details of the data are presented in Table 1. The data sources for this study include official statistical data from the Shanghai municipal statistics bureau, the official website of the Chongming government, the Chongming district statistical yearbook, and the Chongming national economic and social development annual statistical bulletin, covering the period from 2002 to 2022. The data on CO<sub>2</sub> emissions are sourced from the China carbon emission accounts database (CEADs) (Chen et al., 2020). Since CEADs provided Chongming's carbon emission data from 1997 to 2017, this study uses the data from 2002 to 2014 as the training dataset, and the data from 2015 to 2017 as the testing dataset. Ultimately, the model will predict the CO<sub>2</sub> emissions of Chongming from 2018 to 2022 for reference in later studies.

### Data preprocessing

Given the extensive time span of the data and the incompleteness of some data sources due to manual statistics, data preprocessing is essential. In this study, the linear interpolation method is employed to address missing data. Linear interpolation is represented as follows

$$y_t = y_{t-1} + \frac{y_{t+1} - y_{t-1}}{x_{t+1} - x_{t-1}} \cdot (x_t - x_{t-1}) \quad (1)$$

where  $y_t$  represents the missing value, and  $x_t$  represents the time corresponding to the missing value.  $y_{t-1}$  repre-

**Fig. 1** Location of Chongming Island

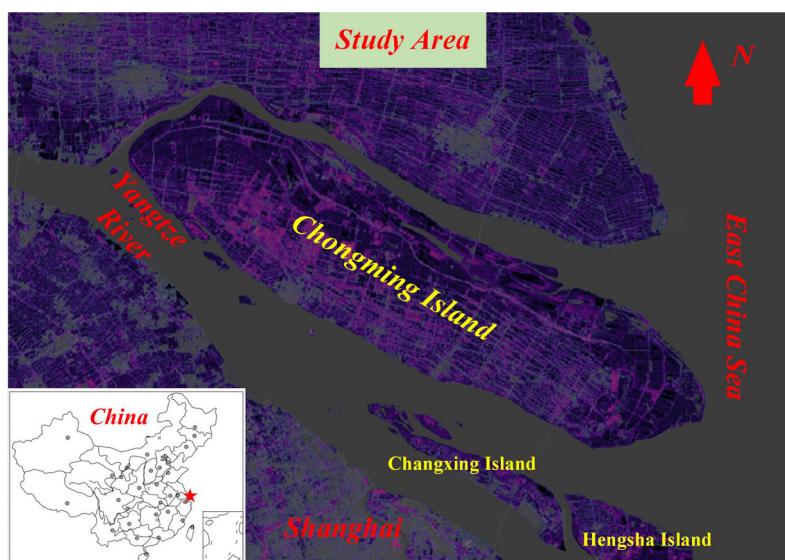


**Table 1** Summary of related indicators, units, and data types

Related indicators	Unit	Data type
Total population	10 thousand people	Socio-economic factors
Natural population growth rate	%	Socio-economic factors
Total added value	10 thousand yuan	Socio-economic factors
Primary industry added value	10 thousand yuan	Socio-economic factors
Secondary industry added value	10 thousand yuan	Socio-economic factors
Tertiary industry added value	10 thousand yuan	Socio-economic factors
Total water supply	Billion cubic meters	Socio-economic factors
Total agricultural output value	10 thousand yuan	Socio-economic factors
Total grain production	Tons	Socio-economic factors
Industrial enterprise revenue	10 thousand yuan	Socio-economic factors
Total industrial profit	10 thousand yuan	Socio-economic factors
Total industrial output of marine equipment industry	10 thousand yuan	Socio-economic factors
Total industrial output of strategic emerging industries	10 thousand tons	Socio-economic factors
Retail sales of consumer goods	10 thousand yuan	Socio-economic factors
Trade fair transaction volume	10 thousand yuan	Socio-economic factors
Fiscal revenue	10 thousand yuan	Socio-economic factors
Fiscal expenditure	10 thousand yuan	Socio-economic factors
Tourist reception number	10 thousand people	Socio-economic factors
Cultivated land area	Hectares	Natural environment
New forest area	Hectares	Natural environment
Forest coverage rate	%	Natural environment
Carbon emission data	10 thousand tons	Natural environment
Total electricity consumption	10 thousand kilowatt-hours	Energy consumption
Industrial coal consumption	10 thousand tons	Energy consumption
Energy consumption per unit GDP	Tons of standard coal per 10 thousand yuan	Energy consumption
Total energy consumption	10 thousand tons of standard coal	Energy consumption

sents the last known value before the missing value, and  $x_{t-1}$  represents the last known time before the missing date.

In this study, min-max normalization is applied, mapping all data to a range of 0 to 1. The calculation is described as follows:

$$x' = \frac{x - x_{\min}}{x_{\max} - x_{\min}} \quad (2)$$

where  $x'$  represents the data after normalization,  $x_{\max}$  is the maximum value of the data, and  $x_{\min}$  is the minimum value of the data.

## Methodology

### Gray correlation analysis

Grey relational analysis is a research methodology utilized for elucidating relationships in the presence of unstable data and unclear information (Ma et al., 2020). The grey correlation can measure the synchronous change relationship between two variables, which we use to find the accounting indicators with a high correlation with Chongming's CO2 emissions prediction. The calculations are as follows. Assume there are multiple analytical objects for the relational variables, each com-



prising multiple analytical factors, forming an attribute matrix pertaining to the analytical factors  $X_{ij}$ .

$$X_{ij} = \begin{bmatrix} x_{11} & \cdots & x_{1n} \\ \vdots & \ddots & \vdots \\ x_{m1} & \cdots & x_{mn} \end{bmatrix} \begin{matrix} i = 1, 2, \dots, m \\ j = 1, 2, \dots, n \end{matrix} \quad (3)$$

where  $X_{ij}$  is the attribute index of the  $i^{th}$  analysis factor of the  $j^{th}$  analysis object. Suppose the reference sequence is set as  $X_0 = [x_0, x_1, \dots, x_n]$ , and the analysis sequence is  $X_{ij}$ , where  $i = 1, 2, \dots, m$ , and  $j = 1, 2, \dots, n$ . The steps of relational analysis are as follows.

(1) Normalize the data using the mean normalization method. Calculate the mean value of the attributes for each analytical object.

$$\bar{x} = \frac{1}{n} \sum_{j=1}^n x_{ij} \quad (4)$$

Preprocess the data using the mean normalization method to ensure comparability between the data.

$$X'_i = \frac{1}{\bar{x}} [x_{i1}, x_{i2}, \dots, x_{ij}, \dots, x_{im}] \quad (5)$$

(2) Calculate the absolute difference between the attributes of each analytical object and the reference object.

$$\Delta_i = |X'_i - X'_0| = [\Delta_{i1}, \Delta_{i1}, \dots, \Delta_{ij}, \dots, \Delta_{in}] \quad (6)$$

(3) Determine the maximum and minimum absolute differences for each analytical object.

$$\Delta_{\max} = \max_i \max_j \Delta_{ij}, \Delta_{\min} = \min_i \min_j \Delta_{ij} \quad (7)$$

(4) Calculate the grey relational coefficient for each analytical object.

$$\eta_i = \frac{\Delta_{\min} + \varphi \Delta_{\max}}{\Delta_j + \varphi \Delta_{\max}} \quad (8)$$

where  $0 \leq \varphi \leq 1$ ,  $\varphi$  is used to enhance the significance of the relational coefficient, typically chosen as 0.5.

(5) Calculate the grey relational degree of the attribute matrix and perform mean normalization on it.

$$\eta = \frac{1}{n} \sum_{i=1}^m \eta_i \quad (9)$$

### DCNN architecture

Owing to its parameter sharing and local receptive fields, CNN excels at extracting spatial features, thereby enhancing the model's perception of spatial data and improving its robustness (Liu et al., 2017). This paper proposes DCNN architecture composed of two channels, each featuring a fully connected layer, dual-channel convolution layer, and pooling layer. The dual-channel convolution layers are configured with varying receptive field sizes to capture both global and

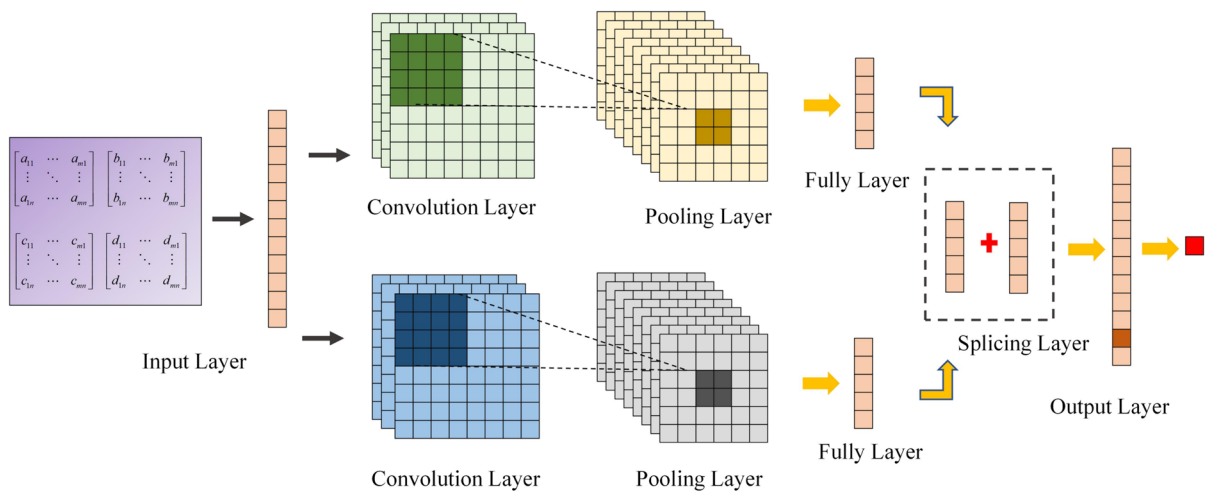


**Fig. 2** DCNN architecture

local features of the accounting indicators. Each channel includes a pooling layer, which serves to reduce redundant features within the channel. Finally, by concatenating the output layers from different channels, the model addresses the lack of correlation between local and global features of carbon emission accounting indicators, thereby generating effective input features for downstream tasks. The structure of DCNN architecture is depicted in Fig. 2.

### GRU network

GRU provides a more efficient method for learning patterns and regularities in sequence data by reducing parameter count, compared to traditional recurrent neural networks and LSTM (Greff et al., 2016). GRU is particularly adept at processing time series data, successfully capturing long-term dependencies in related sequential data such as CO2 emissions. The gating mechanism of GRU, coupled with its reduced parameter count, renders the model highly efficient and accurate. The architecture of the GRU enables it to explore the temporal dependencies of features stacked by DCNN, thereby uncovering the complex spatiotemporal relationships of carbon emissions in Chongming. GRU comprises the update gate, reset gate, and hidden state, among other components.

(1) The update gate is calculated as follows.

$$z_t = \sigma(W_z \cdot [h_{t-1}, x_t] + b_z) \quad (10)$$

(2) The reset gate is calculated as follows.

$$r_t = \sigma(W_r \cdot [h_{t-1}, x_t] + b_r) \quad (11)$$

(3) The candidate's hidden state is as follows.

$$\tilde{h}_t = \tanh(W_h \cdot [r_t \odot h_{t-1}, x_t] + b_h) \quad (12)$$

(4) The new hidden state is as follows.

$$h_t = h_{t-1} \odot z_t + \tilde{h}_t \odot (1 - z_t) \quad (13)$$

where  $h_t$  is the hidden state at time step  $t$ ,  $x_t$  is the input at time step  $t$ ,  $z_t$  is the output of the update gate,  $r_t$  is the output of the reset gate,  $\tilde{h}_t$  is the candidate hidden state,  $\sigma$  the sigmoid function, and  $\odot$  represents element-wise multiplication.  $W_z$ ,  $W_r$ ,  $W_h$  are the weights, and  $b_z$ ,  $b_r$ ,  $b_h$  are the bias terms.

### Comparison of baseline models

This study utilizes multilayer perceptron (MLP), LSTM, and BiLSTM, along with their hybrid combinations, as part of the baseline models for comparison.

The multilayer perceptron (MLP) is a deep learning model based on a feedforward neural network, composed of multiple layers of neurons, where each layer is fully connected to the previous one. Each layer in an MLP consists of numerous neurons: the input layer receives input features, the output layer provides the final prediction, and the hidden layers extract features and perform nonlinear transformations. MLP predicts carbon emissions by learning the relationships between input features (such as economic activities and energy consumption) and CO2 emissions prediction. The MLP can be trained using the backpropagation algorithm, allowing it to automatically learn features and patterns. The structure of the MLP is illustrated in the figure below (Fig. 3).

LSTM can effectively simulate and predict carbon emission trends over time, understanding past and future emission patterns. Each LSTM unit is divided into a forget gate, input gate, selection gate, and output gate. The function of each gate is as follows.

(1) The forget gate decides whether to discard data, implemented through the sigmoid function.

$$f_t = \sigma(W_{if}x_t + b_{if} + W_{hf}h_{t-1} + b_{hf}) \quad (14)$$

The output is 0 or 1, where 0 means to forget and 1 means to retain the memory.

(2) The input gate determines the update value via the sigmoid function.

$$i_t = \sigma(W_{ii}x_t + b_{ii} + W_{hi}h_{t-1} + b_{hi}) \quad (15)$$

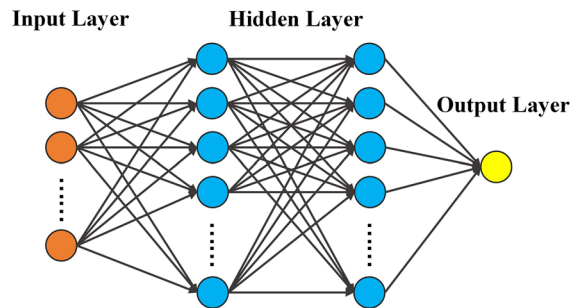
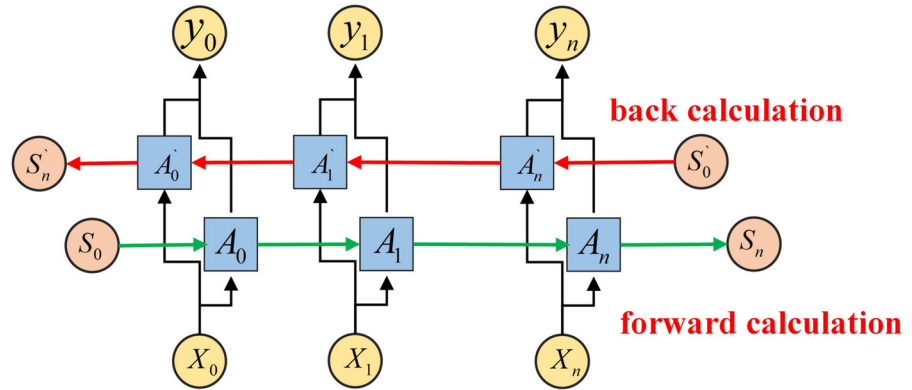


**Fig. 3** MLP architecture

**Fig. 4** BiLSTM architecture



(3) The selection gate is defined as  $g_t$ .

$$g_t = \tanh(W_{ig}x_t + b_{ig} + W_{hg}h_{t-1} + b_{hg}) \quad (16)$$

During each unit's process, the cell state is defined as  $c_t$ , it is the updated value from the previous state  $c_{t-1}$ ,

$$c_t = f_t \times c_{t-1} + i_t \times g_t \quad (17)$$

(4) The LSTM output gate uses the sigmoid function to determine the output value of the cell state,

$$o_t = \sigma(W_{io}x_t + b_{io} + W_{ho}h_{t-1} + b_{ho}) \quad (18)$$

The final output state is  $h_t$ .

$$h_t = o_t \times \tanh(c_t) \quad (19)$$

BiLSTM extends the basic LSTM by incorporating a reverse layer for bidirectional reading. It utilizes two LSTM networks, one processing the input sequence in a forward direction and the other in reverse. This configuration allows each LSTM unit to access contextual information from both preceding and following data at each time step. BiLSTM is particularly suited for carbon emission forecasting that requires learning patterns from both historical and future data, offering a more comprehensive temporal dynamic analysis than unidirectional LSTM. The structure of the BiLSTM is illustrated in Fig. 4.

Structure of the proposed hybrid model

The proposed hybrid model architecture is shown in Fig. 5. This study establishes the GDCNN-GRU hybrid model, which combines grey relational analysis, GRU,

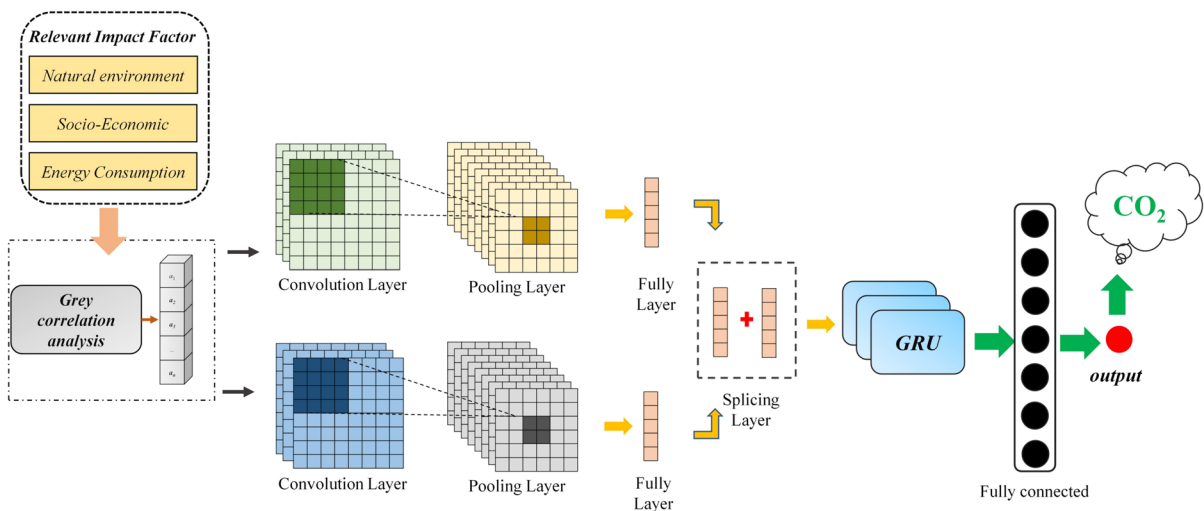


**Fig. 5** Structure of the proposed hybrid model



and DCNN modules to predict the CO<sub>2</sub> emissions intensity of Chongming. Initially, the factors influencing CO<sub>2</sub> emissions are input into the grey relational analysis module to obtain data on highly correlated factors. Subsequently, the obtained factor data is input into the DCNN module to identify local and global spatial features of the factors and their superposition. Following this, the superimposed features are transmitted to the GRU module to calculate the temporal dependencies of the features. Ultimately, the fully connected layer outputs the predicted CO<sub>2</sub> emissions values.

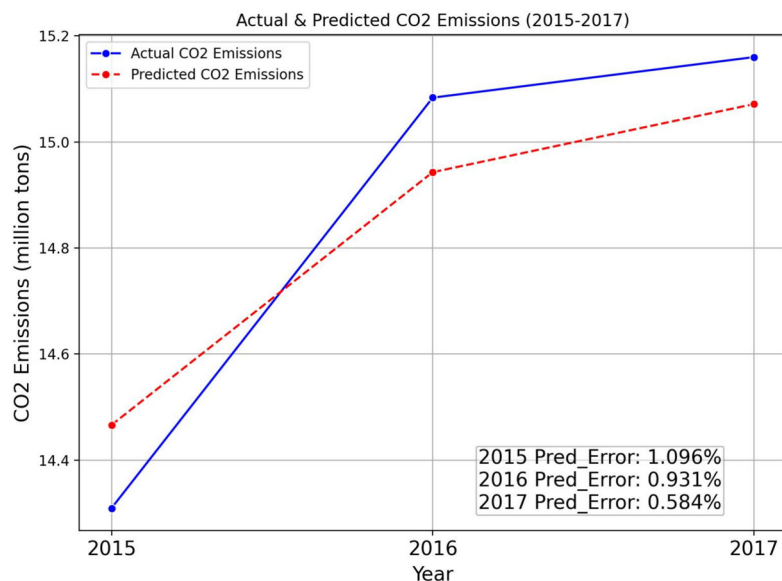
### Model evaluation metrics

Evaluation metrics are methods used to verify the accuracy of model predictions. This study employs mean absolute error (MAE), mean square error (MSE), mean absolute percentage error (MAPE), and coefficient determination (R<sup>2</sup>) to evaluate the performance of the proposed model. Assuming the actual values are  $y_1, y_2, \dots, y_n$  and the predicted values are  $\hat{y}_1, \hat{y}_2, \dots, \hat{y}_n$ , with  $n$  being the number of samples, the calculations for MAE, MSE, MAPE, and R<sup>2</sup> are as follows.

$$MAE = \frac{1}{n} \sum_{t=1}^n |y_t - \hat{y}_t| \quad (20)$$

$$MSE = \frac{1}{n} \sum_{t=1}^n (y_t - \hat{y}_t)^2 \quad (21)$$

**Fig. 6** Analysis of predicted results of Chongming carbon emission for 2015–2017



$$MAPE = \frac{1}{n} \sum_{t=1}^n \left| \frac{y_t - \hat{y}_t}{y_t} \right| \quad (22)$$

$$R^2 = 1 - \sum_{t=1}^n \frac{(y_t - \hat{y}_t)^2}{(y_t - \bar{y}_t)^2} \quad (23)$$

### Model parameter setting

This study evaluates the performance of the proposed model. The dataset used in the model includes Chongming's carbon emission data from 2002 to 2017, along with annual related accounting indicators. The data were subjected to min-max normalization and linear interpolation to ensure consistency and enhance model performance. During training, the Adam optimizer was used with a dynamic learning rate adjustment strategy, and model performance was assessed using the MSE loss function. To enhance the model's generalization ability, L2 regularization was applied. Early stopping criteria were employed to prevent overfitting, and halting training if there was no improvement in loss continuously. For model comparison, this study utilized individual models such as MLP, CNN, LSTM, BiLSTM, and GRU, hybrid models composed of individual models, and hybrid models combining individual models with grey relational analysis as baseline models, confirming the superiority of the proposed model structure. To optimize all models and methods, grid search was used for parameter tuning. Adjustable parameters

included the number of iterations, experimental rounds, training duration, batch size, number of model layers, activation functions, and the number of neurons, among others. The experiments were conducted on a system equipped with an Nvidia 4080 GPU, 24-core Xeon CPU, 64 GB of RAM, and 16 GB of VRAM. All models were developed using the PyTorch 1.9.1 framework and Python 3.8.

## Experimental results and analysis

### Analysis of predicted results

This study predicted CO<sub>2</sub> emissions in Chongming from 2015 to 2017, as shown in Fig. 6. The data indicate that the actual emissions were 14.31 thousand tonnes in 2015 with a prediction of 14.47 thousand tonnes; in 2016, actual emissions reached 15.08 thousand tonnes compared to a predicted 14.94 thousand tonnes; in 2017, emissions were 15.16 thousand tonnes against a forecast of 15.07 thousand tonnes. The comparison results show that the model proposed in this study achieved minimal errors between the predicted and actual CO<sub>2</sub> emissions for 2015 to 2017, specifically 1.096%, 0.931%, and 0.584%, respectively. Employing grey relational analysis and incorporating GRU networks into DCNN effectively captured the temporal data relationships of carbon emission accounting indi-

cators. The CO<sub>2</sub> emission predictions for Chongming demonstrated excellent fitting results, and the hybrid model exhibited robust predictive capabilities.

### Comparison of prediction results with different single models

To validate the proposed model's effectiveness, this study employed MLP, CNN, LSTM, BiLSTM, and GRU as baseline single models to predict CO<sub>2</sub> emissions from 2015 to 2017, with the predictions illustrated in Fig. 7. All baseline models were fine-tuned using hyperparameter optimization techniques to ensure optimal outcomes. The predictive data reveal that the GDCNN-GRU model exhibits greater consistency and accuracy compared to the other single models. Although the LSTM and GRU models performed stably, they did not surpass the predictive accuracy of the GDCNN-GRU. The best-performing MLP model still did not outperform the GDCNN-GRU model. These figures adequately reflect the adaptability and reliability of GDCNN-GRU in predictions, also corroborating its superiority in handling spatio-temporal data.

The models were assessed using metrics such as MAE, MSE, MAPE, and R<sup>2</sup>, with the results detailed in Table 2. Evaluation results indicate that the GDCNN-GRU model demonstrated higher precision and reliability across all key performance indicators compared to the baseline models MLP, CNN, LSTM, BiL-

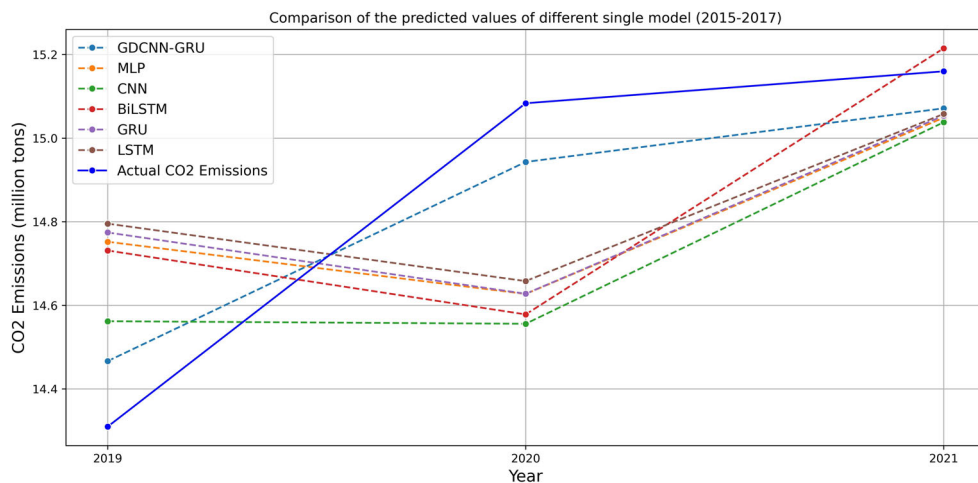


**Fig. 7** Prediction results of different single models

**Table 2** Evaluation results for different single models

Model	MSE	MAE	MAPE	R2
MLP	0.0022	0.0385	4.9626	0.0868
CNN	0.0018	0.0339	4.2773	0.2259
BiLSTM	0.0023	0.0416	5.3123	0.0149
GRU	0.0023	0.0435	5.5699	0.0171
LSTM	0.0023	0.0429	5.5161	0.0341
GDCNN-GRU	0.0006	0.0231	2.9312	0.7463

STM, and GRU. Specifically, the GDCNN-GRU model achieved MSE = 0.0006, MAE = 0.0231, MAPE = 2.931, and R2 = 0.746, outperforming the other models. This data clearly demonstrates the proposed model's predictive accuracy advantage, especially in terms of the R2 value, which indicates superior model fit and predictive efficacy.

#### Comparison of the performance of different hybrid models

To demonstrate the effectiveness of the proposed hybrid model architecture, two hybrid model scenarios are constructed in this section. The first scenario is to compare the performance of the CNN-LSTM, CNN-GRU, and DCNN-GRU hybrid models without grey relational analysis (with a feature count of 26). The second case is the combination of all models and grey analysis to form a hybrid model. The number of features used for grey relational analysis in all models is the best result obtained by iterating over all parameters. The performance analysis of the hybrid models is shown

**Table 3** Comparison of the performance of different hybrid models

Model	Features	MSE	MAE	MAPE	R2
DCNN-GRU	26	0.0007	0.0240	2.9507	0.7003
CNN-GRU	26	0.0022	0.0378	4.9708	0.0896
CNN-LSTM	26	0.0024	0.0446	5.7641	0.0070
Grey-BiLSTM	18	0.0016	0.0314	4.1450	0.3327
Grey-LSTM	18	0.0018	0.0376	4.8821	0.2594
Grey-MLP	18	0.0009	0.0249	3.2549	0.6065
Grey-CNN	12	0.0009	0.0242	3.1131	0.6328
Grey-CNN-GRU	18	0.0019	0.0359	4.7191	0.1900
Grey-CNN-LSTM	11	0.0023	0.0451	5.7942	0.0171
GDCNN-GRU	9	0.0006	0.0231	2.9312	0.7463

in Table 3, and the prediction results are illustrated in Fig. 8.

The table shows that without grey relational analysis, DCNN-GRU already demonstrates strong performance with an MSE of 0.0007 and an R2 of 0.7003, surpassing other baseline models such as CNN-GRU and CNN-LSTM. After employing grey relational analysis, the number of features used in the hybrid models was further reduced. For instance, Grey-CNN-GRU was reduced to 18 features, and Grey-CNN-LSTM used 11 features, yet both performed worse on various evaluation metrics compared to GDCNN-GRU. GDCNN-GRU significantly reduced the number of irrelevant features without sacrificing performance, instead enhancing both efficiency and accuracy. Compared to other hybrid models, GDCNN-GRU reduces data redundancy while improving predictive accuracy. This efficient predictive capability stems from GDCNN-GRU's profound understanding and effective processing of both local and global correlations among accounting indicators and temporal features, enabling it to stand out among similar hybrid models and possess a broader range of applications.

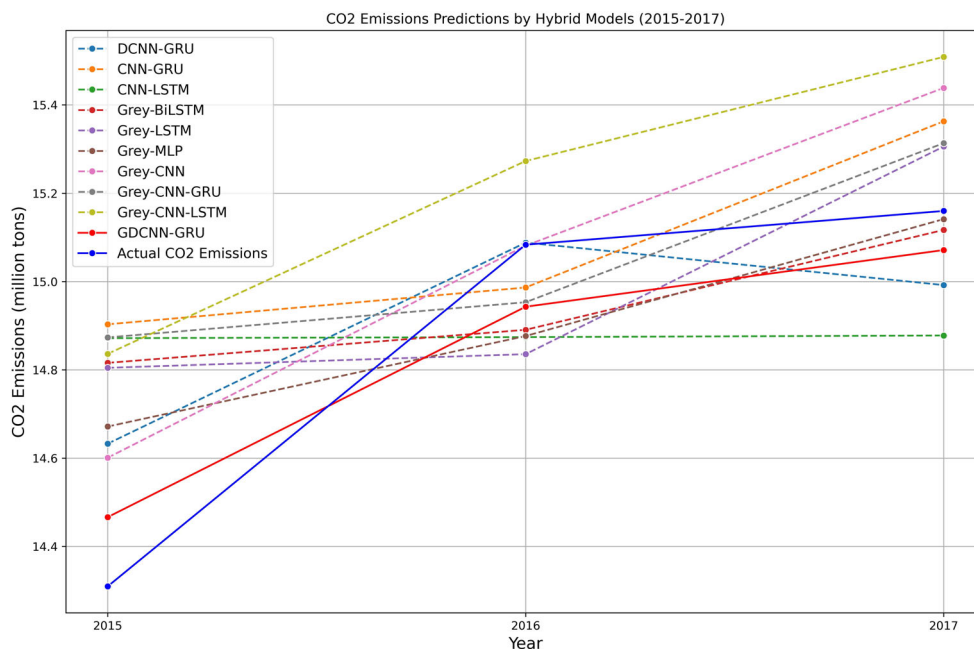


**Fig. 8** Prediction results of different hybrid models

#### Analysis of model-driven capabilities for different data types

CO2 emissions in Chongming, arise from the combined effects of multiple factors, each combination impacting the forecasting results differently. Utilizing comparative experiments and drawing on the classification results from Table 1, this study analyzes how data from various sources affect the prediction results. Here, D1 represents data related to the natural environment; D2 represents energy consumption data; D3 represents socio-economic data; D4 represents a combination of natural environment and energy consumption data; D5 represents natural environment and socio-economic data; and D6 represents socio-economic and energy consumption data. The experimental results are displayed in Fig. 9.

This study analyzed the impact of different data types and their combinations on the performance of CO2 emission prediction models. The analysis revealed that single data types, specifically energy consumption data (D2), showed low predictive accuracy ( $MSE = 0.0058$ ,  $MAE = 0.1112$ ,  $MAPE = 6.718$ ,  $R^2 = 0.0059$ ), indicating that the simplicity of energy data lacks the

complexity required for making accurate predictions. Socio-environmental (D3) and natural environmental data (D1) yielded relatively better predictions. It is evident that single data sources may not suffice for accurate predictions of CO2 emissions in Chongming.

In terms of data combinations, the fusion of natural environment and energy consumption data (D4) and the combination of natural and socio-environmental data (D5) exhibited higher predictive accuracy. Specifically, the D4 combination resulted in  $MSE = 0.0016$ ,  $MAE = 0.0322$ ,  $MAPE = 4.233$ ,  $R^2 = 0.3243$ , whereas the D5 combination demonstrated superior performance ( $MSE = 0.0004$ ,  $MAE = 0.0153$ ,  $MAPE = 2.039$ ,  $R^2 = 0.8226$ ). These results represent the effectiveness of combining natural and socio-environmental data in predicting CO2 emissions in Chongming, also reflecting the critical role of social production and environmental modification in ecological sustainability and CO2 emission predictions. Moreover, the experiment underscores the necessity of integrating multiple data sources, as hybrid network models can effectively leverage the complementarity of various data types to enhance the accuracy and practicality of the models.

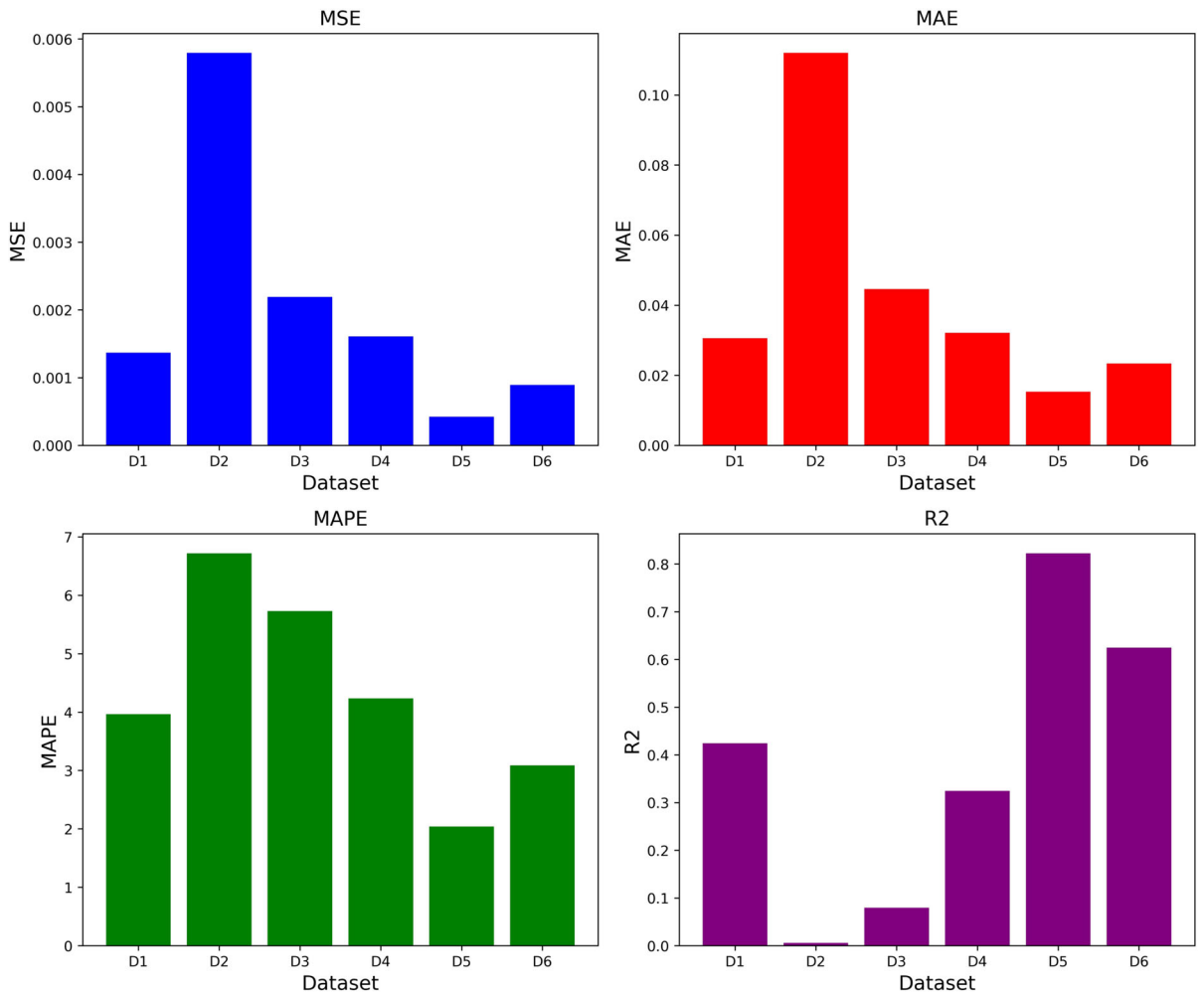


**Fig. 9** Effect of different types of data on prediction evaluation

Comparison with advanced models

To confirm the superiority of the proposed model combination in carbon emission prediction, this study compared it with existing advanced research. Liu et al. (2023b) proposed a prediction algorithm that com-

bins the gray correlation method with the ATT-CNN-LSTM model to forecast carbon emissions in Zhejiang Province from 2022 to 2030. The ATT-CNN-LSTM was trained by analyzing carbon emissions and their influencing factors in Zhejiang Province from 2001 to 2017 to develop a more accurate prediction model. In

**Table 4** Model performance comparison with range and average metrics

Model	Metric	MSE	MAE	MAPE	R2
GDCNN-GRU	Range	[0.0003, 0.0009]	[0.0162, 0.0288]	[2.065, 3.6586]	[0.6104, 0.8831]
	Avg	0.0006	0.0231	2.9312	0.7463
ATT-CNN-LSTM	Range	[0.0023, 0.0024]	[0.0449, 0.0486]	[5.597, 5.9833]	[0.009, 0.128]
	Avg	0.0023	0.0463	5.8957	0.0091



this study, the same methodology as above model was employed to construct the ATT-CNN-LSTM network, and identical parameter settings were applied to the model as described in their paper. The model was run 5 times, and the results of the prediction evaluation are presented in Table 4.

The experimental results demonstrate the exceptional stability of the model proposed in this study. The GDCNN-GRU model's MSE ranged from 0.0003 to 0.0009, with an average of 0.0006, indicating high predictive accuracy. The MAE ranged from 0.0162 to 0.0288, with an average of 0.0231, further validating the consistency and reliability of its predictions. Additionally, the MAPE varied from 2.065 to 3.6586, with an average of 2.9312, showing a lower percentage of prediction error. The R<sup>2</sup> values ranged from 0.6104 to 0.8831, with an average of 0.7463, indicating good explanatory power and fit of the model to the data. In contrast, the performance of the ATT-CNN-LSTM model was inferior. It is worth mentioning that the R<sup>2</sup> values of the ATT-CNN-LSTM model only varied from 0.009 to 0.128, with an average of 0.0091, demonstrating the model's low fitting and explanatory capabilities in the Chongming prediction task. Therefore, the GDCNN-GRU model significantly outperforms the ATT-CNN-LSTM model on several key performance indicators, demonstrating higher prediction accuracy and data-fitting capabilities.

### Chongming CO<sub>2</sub> emissions forecast for 2018–2022

The above experimental results show that the GDCNN-GRU model demonstrates higher accuracy and is well-suited for predicting CO<sub>2</sub> emissions in Chongming. Figure 10 presents the trend of CO<sub>2</sub> emissions in Chongming from 2018 to 2022. The trend of carbon emissions in Chongming from 2018 to 2022 has shown a significant increase, mainly due to the recent development of marine equipment, food processing, and technology-intensive industries, as well as accelerated urbanization. This conclusion is supported by Guo et al. (2023), where Guo et al. analyzed the spatial distribution of carbon emissions in Chongming using nighttime light data and land use data, showing that both the spatial extent and the volume of emissions increased from 2002 to 2020. However, with industrial transformation and ecological development in Chongming, the gap between carbon emissions and carbon sequestration is narrowing, with the model predicting a downward trend in emissions after 2021, showing a 0.6% decrease in 2022 compared to 2021. This finding is consistent with objective laws and is primarily due to the effective measures taken in Chongming to reduce CO<sub>2</sub> emissions; this conclusion has also been validated Zhang et al. (2024).

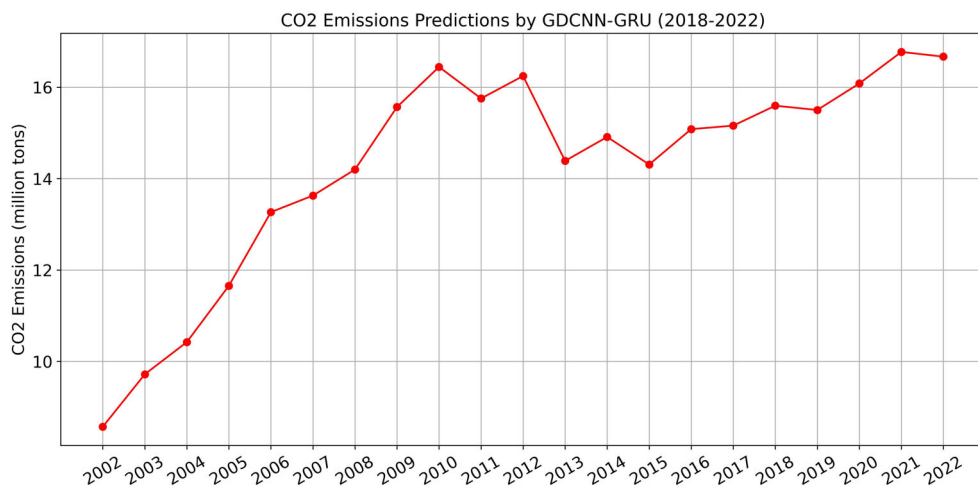


**Fig. 10** Chongming CO<sub>2</sub> emissions forecast for 2018–2022

## Conclusion

Considering the complexity and uncertainty of the factors affecting CO<sub>2</sub> emissions in the Chongming area, this study combined grey relational analysis with a dual-channel CNN and GRU to develop a hybrid prediction model named GDCNN-GRU, which was validated through empirical analysis. The main conclusions of this paper are summarized as follows: (1) Grey theory was utilized to identify the key factors significantly impacting CO<sub>2</sub> emissions among numerous complex factors. (2) The proposed hybrid model integrates local and global features for CO<sub>2</sub> emission accounting metrics in Chongming. It also considers the interactions between spatial features and temporal dependencies, exploring the complex nonlinear relationships between CO<sub>2</sub> emissions in Chongming and various influencing factors through spatiotemporal feature analysis. (3) The model successfully predicted the CO<sub>2</sub> emissions in Chongming from 2018 to 2022, with results consistent with related existing studies. This demonstrates that the proposed model is suitable for predicting CO<sub>2</sub> emissions in Chongming, addressing issues such as the scarcity of effective accounting data and the inaccuracy of traditional calculation methods in regional emission predictions. It suggests that the model has the potential for broader application in regional emission efforts, offering effective guidance for local government decision-making.

Although the model proposed in this study has high predictive accuracy, future research should consider further optimization by: (1) collecting more extensive and larger datasets on factors influencing CO<sub>2</sub> emissions in Chongming to determine if increased data availability can significantly enhance model accuracy and precision; (2) further optimizing model parameters using advanced algorithms and comprehensively assessing their impact on hybrid model performance.

**Acknowledgements** We are particularly grateful to the Institute of Carbon Neutrality of Tongji University for supporting our work.

**Author contributions** Yaqi Wang: supervision, writing—review, methodology, software. Xiaomeng Zhao: conceptualization, investigation. Wenbo Zhu: software, visualization. Yumiao Yin: data management. Jiawei Bi: data management. RenZhou Gui: project management, methodology. All authors reviewed the manuscript.

**Funding** This work was supported by the Science and Technology Innovation Plan of Shanghai Science and Technology Commission (No. 22DZ1209500).

**Data availability** No datasets were generated or analyzed during the current study.

## Declarations

**Ethics approval** All authors have read, understood, and have complied as applicable with the statement on “Ethical responsibilities of Authors” as found in the Instructions for Authors.

**Consent for publication** The authors give the publisher permission to publish the work.

**Conflict of interest** The authors declare no competing interests.

## References

- Ahmadi, M. H., Jashnani, H., Chau, K. W., et al. (2023). Carbon dioxide emissions prediction of five middle eastern countries using artificial neural networks. *Energy Sources, Part A: Recovery, Utilization, and Environmental Effects*, 45(3), 9513–9525.
- Cai, W., Song, X., Zhang, P., et al. (2020). Carbon emissions and driving forces of an island economy: A case study of Chongming Island, China. *Journal of Cleaner Production*, 254, 120028.
- Chen, J., Gao, M., Cheng, S., et al. (2020). County-level co<sub>2</sub> emissions and sequestration in China during 1997–2017. *Scientific Data*, 7(1), 391.
- Ding, S., & Li, R. (2021). Forecasting the sales and stock of electric vehicles using a novel self-adaptive optimized grey model. *Engineering Applications of Artificial Intelligence*, 100, 104148.
- Ding, S., Xu, N., Ye, J., et al. (2020). Estimating Chinese energy-related co<sub>2</sub> emissions by employing a novel discrete grey prediction model. *Journal of Cleaner Production*, 259, 120793.
- Duan, H., He, C., & Pu, S. (2024). A new circular neural grey model and its application to co<sub>2</sub> emissions in China. *Journal of Cleaner Production*, 141318.
- Duan, H., & Pang, X. (2021). A multivariate grey prediction model based on energy logistic equation and its application in energy prediction in China. *Energy*, 229, 120716.
- Faruque, M. O., Rabby, M. A. J., Hossain, M. A., et al. (2022). A comparative analysis to forecast carbon dioxide emissions. *Energy Reports*, 8, 8046–8060.
- Feng, K., Siu, Y. L., Guan, D., et al. (2012). Analyzing drivers of regional carbon dioxide emissions for China: A structural decomposition analysis. *Journal of Industrial Ecology*, 16(4), 600–611.
- Greff, K., Srivastava, R. K., Koutník, J., et al. (2016). LSTM: A search space odyssey. *IEEE Transactions on Neural Networks and Learning Systems*, 28(10), 2222–2232.

- Guo, R., Shao, G., Wu, W., et al. (2023). Analyzing carbon source-sink nexus for green and sustainable transition at the local scale. *Water-Energy Nexus*, 6, 6–12.
- Han, Z., Cui, B., Xu, L., et al. (2023). Coupling LSTM and CNN neural networks for accurate carbon emission prediction in 30 Chinese provinces. *Sustainability*, 15(18), 13934.
- Jiang, M., Huang, Y., Bai, Y., et al. (2023). How can Chinese metropolises drive global carbon emissions? Based on a nested multi-regional input-output model for China. *Science of The Total Environment*, 856, 159094.
- Kang, Y., Mao, S., & Zhang, Y. (2022). Fractional time-varying grey traffic flow model based on viscoelastic fluid and its application. *Transportation Research Part B: Methodological*, 157, 149–174.
- Liao, L., Zhao, C., Li, X., et al. (2021). Towards low carbon development: The role of forest city constructions in China. *Ecological Indicators*, 131, 108199.
- Liu, X., Jin, X., Luo, X., et al. (2023). Quantifying the spatiotemporal dynamics and impact factors of China's county-level carbon emissions using ESTDA and spatial econometric models. *Journal of Cleaner Production*, 410, 137203.
- Liu, W., Wang, Z., Liu, X., et al. (2017). A survey of deep neural network architectures and their applications. *Neurocomputing*, 234, 11–26.
- Liu X, Ye P, Zhao G, et al. (2023b) Prediction of carbon emissions in Zhejiang province based on ATT-CNN-LSTM model. In: *2023 8th Asia Conference on Power and Electrical Engineering (ACPEE)*, IEEE, (pp. 1918–1922)
- Ma, X., Jiang, P., & Jiang, Q. (2020). Research and application of association rule algorithm and an optimized grey model in carbon emissions forecasting. *Technological Forecasting and Social Change*, 158, 120159.
- Muruganandam, M., Rajamanickam, S., Sivarethinamohan, S., et al. (2023). Impact of climate change and anthropogenic activities on aquatic ecosystem-a review. *Environmental Research*, 117233.
- Raza, M. Y. (2022). Towards a sustainable development: Econometric analysis of energy use, economic factors, and co2 emission in Pakistan during 1975–2018. *Environmental Monitoring and Assessment*, 194(2), 73.
- Saleh, C., Dzakiyullah, N. R., Nugroho, J. B. (2016). Carbon dioxide emission prediction using support vector machine. In: *IOP conference series: materials science and engineering*, IOP Publishing, (pp. 012148)
- Song, C., Wang, T., Chen, X., et al. (2023). Ensemble framework for daily carbon dioxide emissions forecasting based on the signal decomposition-reconstruction model. *Applied Energy*, 345, 121330.
- Tong, M., Qin, F., & Duan, H. (2022). A novel optimized grey model and its application in forecasting co2 emissions. *Energy Reports*, 8, 14643–14657.
- Wang, K., Chen, S., Liu, L., et al. (2018). Enhancement of renewable energy penetration through energy storage technologies in a CHP-based energy system for Chongming, China. *Energy*, 162, 988–1002.
- Wang, C., Li, M., & Yan, J. (2023). Forecasting carbon dioxide emissions: Application of a novel two-stage procedure based on machine learning models. *Journal of Water and Climate Change*, 14(2), 477–493.
- Wang, M., Wu, L., & Guo, X. (2022). Application of grey model in influencing factors analysis and trend prediction of carbon emission in Shanxi province. *Environmental Monitoring and Assessment*, 194(8), 542.
- Wang, H., & Zhang, Z. (2022). Forecasting Chinese provincial carbon emissions using a novel grey prediction model considering spatial correlation. *Expert Systems with Applications*, 209, 118261.
- Wen, L., Zhang, J., & Song, Q. (2022). A scenario analysis of Chinese carbon neutral based on STIRPAT and system dynamics model. *Environmental Science and Pollution Research*, 29(36), 55105–55130.
- Wu, S., Zeng, X., Li, C., et al. (2023). Co2 emission forecasting based on nonlinear grey Bernoulli and BP neural network combined model. *Soft Computing*, 27(21), 15509–15521.
- Xu, Y., Lin, T., Du, P., et al. (2024). The research on a novel multivariate grey model and its application in carbon dioxide emissions prediction. *Environmental Science and Pollution Research*, 31(14), 21986–22011.
- Yu, L., Ma, X., Wu, W., et al. (2021). A novel elastic net-based NGBMC (1, n) model with multi-objective optimization for nonlinear time series forecasting. *Communications in Nonlinear Science and Numerical Simulation*, 96, 105696.
- Zeng, S., & Yi, C. (2023). A study of the potential for peak carbon dioxide emissions in metropolitan areas: The case of China. *Environmental Monitoring and Assessment*, 195(6), 787.
- Zhang, Y., Guo, R., Peng, K., et al. (2024). Carbon neutrality transformation pathway in ecoregions: an empirical study of Chongming district, Shanghai, China. *Water-Energy Nexus*
- Zhang, X., Yan, F., Liu, H., et al. (2021). Towards low carbon cities: A machine learning method for predicting urban blocks carbon emissions (UBCE) based on built environment factors (BEF) in Changxing City, China. *Sustainable Cities and Society*, 69, 102875.
- Zhou, W., Zeng, B., Wang, J., et al. (2021). Forecasting Chinese carbon emissions using a novel grey rolling prediction model. *Chaos, Solitons & Fractals*, 147, 110968.

**Publisher's Note** Springer Nature remains neutral with regard to jurisdictional claims in published maps and institutional affiliations.

Springer Nature or its licensor (e.g. a society or other partner) holds exclusive rights to this article under a publishing agreement with the author(s) or other rightsholder(s); author self-archiving of the accepted manuscript version of this article is solely governed by the terms of such publishing agreement and applicable law.